Heliyon 8 (2022) e10750

Contents lists available at ScienceDirect

Heliyon

journal homepage: www.cell.com/heliyon

Research article

Leucine zipper protein 2 serves as a prognostic biomarker for prostate cancer correlating with immune infiltration and epigenetic regulation

Dechao Feng [1], Weizhen Zhu [1], Xu Shi [1], Wuran Wei, Ping Han, Qiang Wei [**], Lu Yang [*]

Department of Urology, Institute of Urology, West China Hospital, Sichuan University, Chengdu 610041, China

ARTICLE INFO

Keywords:
Prostate cancer
Senescence
Tumor immune environment
RNA modification
DNA methylation
Leucine zipper protein 2

ABSTRACT

Background: We sought to determine whether leucine zipper protein 2 (LUZP2) could benefit men with prostate cancer (PCa) undergoing radical radiotherapy (RT) or prostatectomy (RP).

Methods: Analysis was done on differentiating expression, clinical prognosis, co-expressed genes, immune infiltration, and epigenetic changes. All of our analyses were done using the R software (version 3.6.3) and the appropriate packages.

Results: In terms of PCa, tumor samples expressed LUZP2 more than normal samples did. In the TCGA database and GSE116918, we found that LUZP2 was the only independent risk factor for PCa. The shared enriched pathways for patients undergoing RP or RT were cell-cell adhesion, regulation of filopodium assembly, and extracellular matrix containing collagen. With the exception of TNFRSF14, we discovered that LUZP2 was negatively correlated with 21 immune checkpoints in PCa patients receiving RT. We found a significant inverse relationship between LUZP2 expression and the tumor immune environment, which included B cells, CD4+ T cells, neutrophils, macrophages, dendritic cells, stromal score, immune score, and estimate score, in patients receiving RP or RT. Additionally, tumor purity was positively correlated with LUZP2. We found that the drug bortezomib may be susceptible to the LUZP2. DNA methylation was significantly associated with the mRNA expression of LUZP2 in PCa patients from the TCGA database, and LUZP2 methylation was positively correlated with immune cells. The proliferative activity of various PCa cells, which correlated to different stages of this disease, was also found to be significantly reduced by LUZP2 reduction, according to the results of our experimental work.

Conclusions: We proposed a relatively comprehensive understanding of the roles of LUZP2 on PCa from the fresh perspective of senescence.

1. Introduction

According to the most recent cancer statistics [1,] prostate cancer (PCa) is the leading cause of tumor morbidity in men worldwide. Despite having a 5-year survival rate of up to 98%, PCa cancer-specific mortality accounted for 11% of all male malignant tumor-related fatalities [2]. Currently, active surveillance, radical prostatectomy (RP) or radical radiotherapy (RT), androgen deprivation therapy, and chemotherapy are used to treat PCa, depending on clinical stages, Gleason score, patient performance, and life expectancy [3]. RP or RT are the preferred approaches for patients with localized PCa, with biochemical recurrence (BCR) occurring in 27%–53% of RP patients and 10–70% of RT patients, respectively [4, 5]. Men over the age of 65 are more likely to develop PCa, and by 2050, nearly twice the current population (over 1.5 billion people) will be over the age of 65 [2,6]. PCa is an age-related disease whose social conundrum can be exacerbated by global population aging [7].

The role of senescence is attracting considerable critical attention in a variety of fields. Senescent cells exhibit a failure to re-enter the cell cycle in response to mitogenic stimuli, an enhanced secretory phenotype, and resistance to cell death in a variety of tissues during physiological and pathological processes such as tissue remodeling, injury, cancer, and aging [8]. As a result, senescence acts as a strong barrier to tumorigenesis in cancers, and inducing senescence in cancer cells may be a potentially

* Corresponding author.
** Corresponding author.
E-mail addresses: weiqiang933@126.com (Q. Wei), wycleflue@scu.edu.cn (L. Yang).
[1] These authors contributed equally to this work.

https://doi.org/10.1016/j.heliyon.2022.e10750
Received 11 July 2022; Received in revised form 19 August 2022; Accepted 20 September 2022

therapeutic approach [8]. PCa and aging are linked in a subtle way. In contrast to other organs, prostate tissue does not lose tissue mass or its ability to regenerate as it ages. Instead, its volume is increasing [9]. PCa is an age-related disease, and from the standpoint of senescence, leucine zipper protein 2 (LUZP2) was identified as a potential target of PCa via a senescence-related database (SeneQuest, http://Senequest.net) [10].

LUZP2 is found on Chr11p13–11p14 and encodes a leucine zipper protein, the deletion of which has been linked to low grade glioma, Alzheimer's disease, and schizophrenia [11, 12, 13, 14, 15]. Zhao et al. [16] investigated the expression of androgen receptor-regulated enhancer RNAs and associated mRNAs in the FTO, LUZP2, MARC1, and NCAM2 loci in terms of PCa. Surprisingly, they discovered that LUZP2 mRNA expression was higher in primary tumors than in normal prostate tissues, but decreased again in metastatic castration-resistant PCa [16]. However, no detailed study of LUZP2 in PCa has been conducted thus far. We investigated the potential role of LUZP2 in PCa patients undergoing radical prostatectomy (RP) or radical radiotherapy (RT) in this study. Our research has been submitted to the ISRCTN registry (No. ISRCTN11560295).

2. Methods

2.1. Cell lines and reagents

Human normal prostate epithelial cell (RWPE-1) was purchased from Zhongqiao Xinzhou (https://www.zqxzbio.com/Index/p_more/pid/779.html) and cultured in matched keratinocyte complete medium. Human normal prostate stromal cell (WMPY-1) was purchased and authenticated from cell bank (Chinese Academy of Sciences, Shanghai, China) and cultured in DMEM (Invitrogen, CA, United States) with 10% fetal bovine serum (FBS) (CxCell BIO, Uruguay). Human PCA cell lines, LNCap, PC3 and DU145, were purchased and authenticated from cell bank (Chinese Academy of Sciences, Shanghai, China). Human PCA cell lines, C4-2 and C4–2B were purchased from BNCC (https://www.bncc.org.cn/). LNCap, C4-2, C4–2B and DU145 were cultured in RPMI medium 1640 (Gibco) with 10% FBS and 5% penicillin-streptomycin solution. PC3 was cultured in DMEM/F12 (Gibco) with 10% FBS and 5% penicillin-streptomycin solution. All cells were incubated in 5% CO2 incubator at 37 °C and were tested for mycoplasma free via a mycoplasma detection kit (Thermo Fisher Scientific, United States).

2.2. Data collection

Using the R package "inSilicoMerging" [18], we combined four datasets from our previous study [17], including GSE46602 [19], GSE32571 [20], GSE62872 [21], and GSE116918 [22], and removed the batch effects using the "removeBatchEffect" function of R package "limma (version 3.42.2). The mRNA matrix was extracted from the merged datasets, and three datasets [19, 20, 21] containing 360 tumor and 209 normal samples were used to identify the differentially expressed genes (DEGs) defined by llogFCl 0.4 and p. adj. 0.05. Following that, we downloaded standardized PCa data from the UCSC XENA [23], and the above methods were used to proceed with the 498 tumor and 52 normal tissues in the TCGA database to determine the mRNA matrix of DEGs. We discovered the common senescence-related DEGs by combining senescence-related genes [10] and DEGs from the TCGA and GEO datasets [23, 24, 25]. The DEGs associated with biochemical recurrence (BCR)-free survival, namely candidate genes, were identified in 248 PCa patients undergoing RT in the GSE116918 [22] database and 430 PCa patients undergoing RP in the TCGA database. Through univariate and multivariate COX regression analysis, we were able to identify the independent risk gene (LUZP2) for PCa patients undergoing RP or RT. We investigated the clinical correlations of LUZP2 in the TCGA database and GSE116918 [22], as well as the differential expression of LUZP2 in pan cancer using the TIMER 2.0 [24].

2.3. Genetic correlation and functional enrichment analysis

The above DEGs were used to identify genes related to LUZP2 using Spearman analysis (p 0.001), which was then used to conduct a Gene ontology (GO) analysis to investigate possible biological functions and signaling pathways affected by LUZP2 [25]. Biological process (BP), cell composition (CC), and molecular function (MF) were all included in the GO analysis (MF). The PCa patients in the TCGA database or GSE116918 [22] were divided into two groups based on the median expression of LUZP2. The GSEA was then performed using "c2. cp.kegg.v7.4. symbols.gmt" from the molecular signatures database [26]. P. adjust = 0.05 and false discovery rate = 0.25 were considered statistically significant.

2.4. RNA modifications and tumor immune environment (TME)

The Spearman correlation analysis was used to investigate the relationship between the expression of LUZP2 and RNA modification-related genes (m1A, m5C, and m6A). Using the Timer and Estimate algorithms, a similar analysis was performed for checkpoints and immune parameters [27, 28]. We investigated LUZP2 drug sensitivity using GSCALite, which included data from the genomics of drug sensitivity in cancer (GDSC) [29]. Furthermore, we used Spearman analysis to investigate the relationship between DNA methylation and LUZP2 mRNA expression. The TISIDB database was also used to investigate the relationship between tumor infiltrating lymphocytes and LUZP2 expression or methylation [30].

2.5. Real-time quantitative polymerase chain reaction (RT-qPCR)

Total RNA from prostate cells were extracted using the animal total RNA isolation kit (www.foregene.com), and cDNA was synthesized using the iScript advanced cDNA synthesis kit (BioRad). RT-qPCR analysis was performed using the real time PCR easy™-SYBR Green I (FOREGENE, Cat. No. QP-01011/01012/01013/01014) according to the manufacturer's instructions. Glyceraldehyde-3-phosphate dehydrogenase (GAPDH) was used as an internal control. GAPDH: 5′- CTGGGCTACACTGAGCACC-3' (forward) and 5′-TCC AAGTGGTCGTTGAGGGCAATG-3' (reverse); LUZP2: 5′- AGCAGCTCTTGACAGGGAGT-3' (forward) and 5′-GTGGGAGTAACATCCGAGTTG-3' (reverse).

2.6. Small interfering RNA (siRNA) of LUZP2 and cell proliferation

siRNA was designed by HIPPOBIO (www.hippobiotec.com). LUZP2 si-1sense: 5′- CGUGUUCCAUGAAGCACAAdTdT-3'; LUZP2 si-1 antisense: 5′- UUGUGCUUCAUGGAACACGdTdT-3'. LUZP2 si-2 sense: 5′-GAAUUAGGACAGAAACAAAdTdT-3'; LUZP2 si-2 antisense: 5′- UUUGUUUCUGUCCUAAUUCdTdT-3'; LUZP2 si-3 sense: 5′- GACUAUGAAGAGCUAGAAAdTdT-3'; LUZP2 si-3 antisense: 5′-UUUCUAGCUCUUCAUAGUCdTdT-3'. Prostate cells were transfected using lipofectamine 2000 (Invitrogen) according to the instructions. RT-qPCR was used to determine the effective siRNAs of LUZP2. Through transfection of LUZP2 siRNAs, the effect of LUZP2 on the proliferation of five PCa cell lines was analyzed by cell counting kit-8 (CCK8) assay at 24h, 48h and 72h.

2.7. Statistical analysis

All analyses were carried out using R (version 3.6.3) and the appropriate packages. If the data did not fit the normal distribution, we used the Wilcoxon test. The prognostic value of LUZP2 was evaluated using COX regression analysis. The statistical significance level was set to two-sided p 0.05. The following significance levels were used: no significance (ns), p 0.05; *, p 0.05; **, p 0.01; ***, p 0.001.

3. Results

3.1. Identification of LUZP2 and related clinical values

In the TCGA (Figure 1A) and GEO datasets [27, 28, 29] (Figure 1B), respectively, 6309 and 343 DEGs between PCa and normal tissues were found. The intersection of the above DEGs and 12289 senescence-related genes yielded 266 senescence-related DEGs [18] (Figure 1C). Following that, we identified 12 common DEGs associated with BCR-free survival in PCa patients undergoing RP in the TCGA database and RT in the GSE116918 database [26] (Figure 1D). Finally, we discovered that LUZP2 was an independent risk factor for PCa in both the TCGA database (Figure 1E) and the GSE116918 [22] datasets (Figure 1F). We also looked at LUZP2's clinical correlations and discovered that it was significantly associated with a higher Gleason score in PCa patients undergoing RP ($p = 0.002$, Table 1) rather than those undergoing RT (Table 2). Furthermore, we found that LUZP2 expression was significantly different in most cancers (Figure 1G). In terms of PCa, tumor samples had higher levels of LUZP2 expression than normal samples (Fig. 1A-B and Fig. 1G). The top ten genes associated with LUZP2 in RP patients were TMTC4, GNCT1, CACNA1D, RAB3B, DNAJC10, COL9A2, MYO6, CRISP3, UAP1, and ERG (Figure 1H). The top ten genes associated with LUZP2 in patients undergoing RT were BICD1, CACNA1D, CPNE4, CRISP3, RAB3B, RALGAPA2, SPOCK1, TMTC4, ERG, and MYO6 (Figure 1I).

3.2. Functional enrichment analysis and RNA modifications

The common enriched pathways for patients undergoing RP (Figure 2A) or RT (Figure 2B) were regulation of filopodium assembly, collagen-containing extracellular matrix (ECM), cell-cell adhesion mediator activity, cell adhesion mediator activity, and cadherin binding involved in cell-cell adhesion. Based on the median expression of LUZP2, we divided the PCa patients into high- and low-expression groups. Protein export and aminoacyl tRNA biosynthesis were found to be highly enriched in the high-expression group of PCa patients undergoing RP (Figure 2C). Protein export, ribosome, spliceosome, ubiquitin-mediated proteolysis, and the Notch signaling pathway were found to be highly enriched in the high-expression group of PCa patients undergoing RT (Figure 2D).

For patients undergoing RP, m1A analysis showed that LUZP2 was closely associated with TRMT61A (r: -0.2), TRMT61B (r: 0.16), and YTHDF3 (r: 0.15) (Figure 2E); m5C analysis showed that LUZP2 was highly related to NSUN5 (r: -0.17), DNMT1 (r: -0.1), DNMT3B (r: -0.2), NSUN2 (r: 0.19), NSUN7 (r: 0.35), DNMT3A (r: 0.18), NSUN4 (r: 0.16), TRDMT1 (r: 0.19), NSUN3 (r: 0.2), NSUN6 (r: 0.16), and TET2 (r: 0.13) (Figure 2F); m6A analysis showed that LUZP2 was closely associated with ALKBH5 (r: -0.17), ELAVL1 (r: 0.1), HNRNPC (r: 0.19), LRPPRC (r: 0.24), METTL14 (r: 0.21), RBM15B (r: 0.22), WTAP (r: 0.16), YTHDC2 (r: 0.11), YTHDF3 (r: 0.15), and ZC3H13 (r: 0.11) (Figure 2G).

For patients undergoing RT, m1A analysis showed that LUZP2 was closely associated with TRMT6 (r: 0.14), YTHDC1 (r: 0.19), YTHDF2 (r: 0.13), and YTHDF3 (r: 0.16) (Figure 2H); m5C analysis showed that LUZP2 was closely associated with DNMT3A (r: 0.18), NSUN2 (r: -0.18), and NSUN7 (r: 0.32) (Figure 2I); m6A analysis showed that LUZP2 was closely associated with ELAVL1 (r: 0.14), HNRNPA2B1 (r: 0.22), HNRNPC (r: 0.14), METTL3 (r: 0.13), RBM15B (r: 0.17), YTHDC1 (r: 0.19), YTHDF2 (r: 0.13), and YTHDF3 (r: 0.16) (Figure 2J).

3.3. TME analysis and DNA methylation

Except for CD276 and TNFSF4, the Spearman analysis revealed that LUZP2 was negatively related to 41 immune checkpoints in PCa patients undergoing RP (Figure 3A). Except for TNFRSF14, we discovered that LUZP2 was negatively associated with 21 immune checkpoints in PCa patients undergoing RT (Figure 3B). LGALS9, CD274, KLRD1, ICOSLG, TNFRSF4, VTCN1, CD40, CD70, CD244, PDCD1LG2, TNFRSF18, LAIR1, CD200, HAVCR2, and LAYN were the most common immune checkpoints for PCa patients undergoing RP and RT. We found a significant negative correlation between LUZP2 expression and TME parameters in patients undergoing RP, including B cells (r: -0.18), CD4+ T cells (r: -0.26), neutrophils (r: -0.21), macrophages (r: -0.16), dendritic cells (r: -0.24), stromal score (r: -0.15), immune score (r: -0.23), and estimate score (r (Figure 3C). We found a significant negative correlation between LUZP2 expression and B cells (r: -0.18), CD4+ T cells (r: -0.29), neutrophils (r: -0.3), dendritic cells (r: -0.33), stromal score (r: -0.24), immune score (r: -0.32), and estimate score (r: -0.3) in patients undergoing RT (Figure 3D). Furthermore, we discovered that bortezomib may be a potentially sensitive drug to the LUZP2 (Figure 3E).

DNA methylation analysis of PCa patients from the TCGA database revealed that cg24473393 (r: -0.172; Figure 3F), cg13376598 (r: -0.216; Figure 3G), cg10345326 (r: -0.112; Figure 3H), and cg08068240 (r: -0.093; Figure 3I) were significantly associated with LUZP2 m Furthermore, we discovered that LUZP2 expression was negatively associated with the majority of tumor infiltrating lymphocytes, but LUZP2 methylation produced the opposite results using the TISIDB database [25] (Figure 3J).

3.4. Cell proliferation

We discovered that LUZP2 was highly expressed in LNCap cells but was clearly downregulated in PC3 and DU145 cells (Figure 4A). We discovered that siRNA2 and siRNA3 of LUZP2 could effectively reduce LUZP2 mRNA expression in C4-2 cells using the RT-qPCR assay (Figure 4B). Furthermore, these siRNAs could significantly reduce the ability of LNCap, C4-2, C4–2B, PC3, and DU145 cells to proliferate (Fig. 4C-G).

4. Discussion

Cellular senescence, which has recently been identified as a component of the cancer phenotype, appears to be linked to both degenerative and hyperplastic diseases of aging [8, 31]. Leucine zipper structures are typically found at the C-terminus of eukaryotic DNA binding proteins such as yeast transcription activator GCN4, oncoprotein JUN, FOS, and MYC, all of which have been linked to oncogene expression and regulation functions [32, 33]. PCa biomarkers appear in an endless stream, with many of them being used in translational applications. As a result, we can project our expectations onto LUZP2 [34]. Downregulation of LUZP2 is linked to cellular senescence [5, which has been linked to a number of age-related diseases [13, 14, 15, 16]. Only the brain and the adrenal glands have higher levels of LUZP2 expression [35]. However, the impact of LUZP2 on oncology has received little attention in the research literature. The purpose of this study was to determine the role of LUZP2 in PCa, a serious age-related cancer. We found significantly different expression of LUZP2 in many cancers, including LGG and PCa, which is consistent with previous research [11, 16]. Downregulation of LUZP2 was significantly associated with poor prognosis in PCa patients receiving RP or RT, which was consistent with a previous study finding reduced LUZP2 expression level in metastatic castration-resistant PCa [16]. Furthermore, a previous study found that LUZP2 mRNA expression increased in primary tumors compared to normal prostate tissues but decreased again in metastatic castration-resistant PCa [16]. Our experimental findings supported this conclusion, and we discovered that reducing LUZP2 could significantly reduce the proliferation activity of various PCa cells, which corresponded to different stages of the disease. As a result, LUZP2 may be a prognostic biomarker for PCa patients.

Surprisingly, we discovered that the outcomes of co-expressed genes, functional enrichment analysis, epigenetic modifications, and TME analysis were not exactly the same for the two PCa treatments, namely RP and RT. TMTC4, CACNA1D, RAB3B, MYO6, CRISP3, ERG, CTSB, and ANXA2 were among the genes that interacted with LUZP2. TMTC4, which encodes a transmembrane protein, is a gene associated with

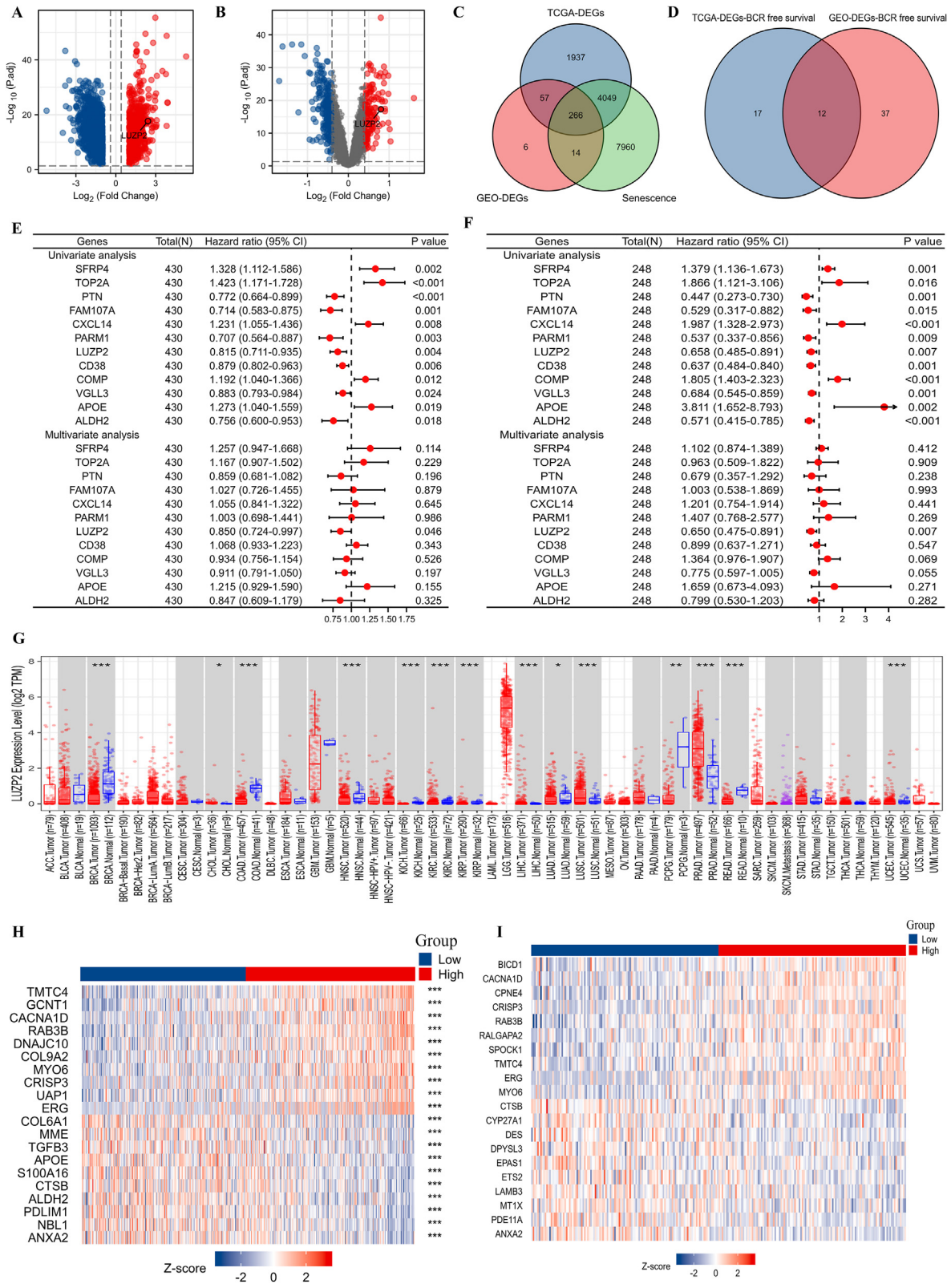

Figure 1. Identification of LUZP2 and co-expressed genes (A) volcano plot displaying DEGs between tumor and normal tissues in the TCGA database; (B) volcano plot displaying DEGs between tumor and normal tissues in the GSE116918 [17]; (C) Venn post displaying the intersection of senescence-related genes and DEGs in the TCGA database and GSE116918 [17] (D) Venn post displaying the intersection of DEGs associated with BCR-free survival in the TCGA database; (F) forest plot displaying the results of COX regression using 12 DEGs associated with BCR-free survival for PCa patients undergoing radical radiotherapy in the GSE116918 [17] (G) the DEGs between tumor and normal tissues in the pan-cancer analysis; (H) heatmap displaying co-expressed LUZP2 genes for PCa patients undergoing radical prostatectomy; (I) heatmap displaying co-expressed LUZP2 genes for PCa. DEGs = differentially expressed genes; BCR = biochemical recurrence; PCa = prostate cancer.

Table 1. The correlation between LUZP2 expression and clinical features in the TCGA database.

Features	LUZP2		P value
	Low expression	High expression	
Samples	215	215	
Age, median (IQR)	61 (55.5, 66)	62 (57, 66)	0.204
Gleason score, n (%)			0.002
GS = 6	23 (5.3%)	16 (3.7%)	
GS = 7	119 (27.7%)	87 (20.2%)	
GS = 8	26 (6%)	33 (7.7%)	
GS = 9	47 (10.9%)	79 (18.4%)	
T stage, n (%)			0.053
T2	88 (20.8%)	67 (15.8%)	
T3	123 (29%)	138 (32.5%)	
T4	2 (0.5%)	6 (1.4%)	
Race, n (%)			0.622
Asian	6 (1.4%)	5 (1.2%)	
Black or African American	28 (6.7%)	22 (5.3%)	
White	174 (41.8%)	181 (43.5%)	
N stage, n (%)			0.359
N0	150 (40%)	156 (41.6%)	
N1	29 (7.7%)	40 (10.7%)	
Residual tumor, n (%)			0.047
No	147 (35.1%)	126 (30.1%)	
Yes	63 (15%)	83 (19.8%)	

IQR: interquartile range; GS: Gleason score.

Table 2. The correlation between LUZP2 expression and clinical features in the GSE116918 [17].

Features	LUZP2		P value
	Low expression	High expression	
Samples	124	124	
Age, median (IQR)	67.5 (63, 72)	68 (63.75, 73)	0.646
T stage, n (%)			0.931
T1	25 (11.2%)	26 (11.7%)	
T2	36 (16.1%)	40 (17.9%)	
T3	48 (21.5%)	44 (19.7%)	
T4	2 (0.9%)	2 (0.9%)	
Gleason score, n (%)			0.152
GS = 6	26 (10.5%)	16 (6.5%)	
GS = 7	43 (17.3%)	56 (22.6%)	
GS = 8	24 (9.7%)	28 (11.3%)	
GS = 9	31 (12.5%)	24 (9.7%)	

IQR: interquartile range; GS: Gleason score.

LUZP2 during surgery and radiotherapy, with 100% and 96.6% sensitivity and specificity for detecting PCa, respectively [36]. Simultaneously, CACNA1D, a gene encoding voltage-gated calcium channels, is thought to be linked to a number of urinary cancers, including aldosterone adenoma and PCa [37, 38]. RAB3B is a gene associated with senescence and the expression of apoptotic proteins, and its expression level is strongly associated with glioma progression [39]. CTSB encodes cathepsin B, a lysosomal cascade component that regulates tumor cell apoptosis, angiogenesis, and metastasis [40]. Furthermore, MYO6, CRISP3, ERG, and ANXA2 have been linked to the prognosis of PCa [41, 42, 43]. Glycosylation is a universal target for androgen control in prostate cancer cells for PCa patients undergoing RP, including GCNT1 and UAP1, both of which are significantly upregulated in prostate cancer tissue [44]. The effects of COL6A2 and DNAJC10 on bladder and breast cancers have been documented [45, 46], but their roles in PCa remain unknown. The roles of SPCOK1, BCD1, and RALGAPA2 in PCa are detected in PCa patients undergoing RT [47, 48, 49], but it is unclear how CPNE4 affects PCa. In our study, we discovered that the functional analysis results were concentrated in the tumor's filopodium assembly, cell adhesion, and ECM, regardless of treatment methods. The combined effect of the three is to promote cell migration, which regulates cancer cells' chemotactic migration to invade surrounding tissues and vasculature [50]. ECM, which includes a number of proteins, is required for tumor cells to absorb nutrients from TME and serves as the primary structural support and physiological barrier for both tumor cells and other types of TME cells [51]. Actin polymerizes filopodia, which adheres to the ECM or adjacent cells via transmembrane receptors [52]. To cross the physical barrier of ECM in tumor tissues, cancer cells form protrusions that have the ability to remodel and degrade ECM. This type of filopodium is known as an invadopodium, and its formation is regulated by chemotaxis and invasion signals, as well as having high proteolytic activity [53, 54, 55]. Sarcomere, which is primarily composed of actin and myosin, is another protein involved in the control of cell mobility and tumor cell metastasis, and its disruption can result in a variety of tumors, including bladder cancer, lung cancer, and glioma [56, 57, 58, 59, 60, 61]. Oncogenes are genes that code for sarcomeres [62]. In conclusion, decreased cell adhesion is one of the morphological characteristics of malignant tumors [63], and the primary function of LUZP2 that affects cancer prognosis may be focused on the decrease in cancer cell adhesion and the increase in motility and migration. Furthermore, we discovered that protein export was a common mechanism in PCa patients with high-expression LUPZ2 who underwent RP or RT, which may be explained by the high consumption of cancer and tissue damage followed by surgery or radiotherapy. Aminoacyl tRNA biosynthesis was significantly enriched in the high-expression group of PCa patients undergoing RP. Aside from translation, aminoacyl tRNA synthetase promotes tumorigenesis by forming a large multi-synthetic enzyme complex, whereas freestanding aminoacyl tRNA synthetase can both promote and inhibit cancer via signal transduction, angiogenesis, nutritional balance, and immune response regulation [64, 65]. However, more diverse pathways were enriched in PCa patients undergoing RT who expressed higher levels of LUZP2. In patients undergoing RP, the ribosome and spliceosome pathways may be similar to the aforementioned aminoacyl tRNA biosynthesis. The major protein degradation systems in eukaryotic cells are autophagy and the ubiquitin-proteasome pathway (UPP), and both have been shown to play a role in tumorigenesis [66]. Furthermore, UPP has been shown to promote senescence, which is tightly regulated by E3 ubiquitin ligases, deubiquitinases, and various post-translational modifications of target proteins [66]. Furthermore, the Notch signaling pathway has been linked to senescence and the senescence-associated secretory phenotype [67, 68, 69].

m6A is the most common RNA modification in eukaryotic cells [70]. LUZP2 was found to be positively correlated with YTHDF3, ELAVL1, RBM15B, and HNRNPC in both RP and RP patients. In addition to YTHDF3 improving target RNA translation efficiency [71], ELAVL1 [72], RBM15B [73], and HNRNPC [74] were found to be negatively regulating mRNA splicing and translation. However, the possible m6A modification effects for the RP or RT groups alone were somewhat unclear. In patients undergoing RP, for example, LUZP2 was found to be positively correlated with WTAP (promotes RNA-binding capability of METTL3 [75]), METTL14 (provides an RNA-binding scaffold [71]), and YTHDC2 (improving target mRNA translation efficiency, but reducing its abundance [76]). Furthermore, METTL14 altered Notch 1, reducing its carcinogenic effect [77]. Furthermore, LUZP2 was found to be negatively associated with ALKBH5, an eraser that promoted mRNA export and translation [78]. Both METTL3 [79] and HNRNPA2B1 [80], which were positively correlated with LUZP2, were translation promoters in patients undergoing RT. The contradictory result could be due to differences in treatment methods. M1A and m5C play only a minor role in RNA modification [70]. It has been demonstrated that the YTH protein family

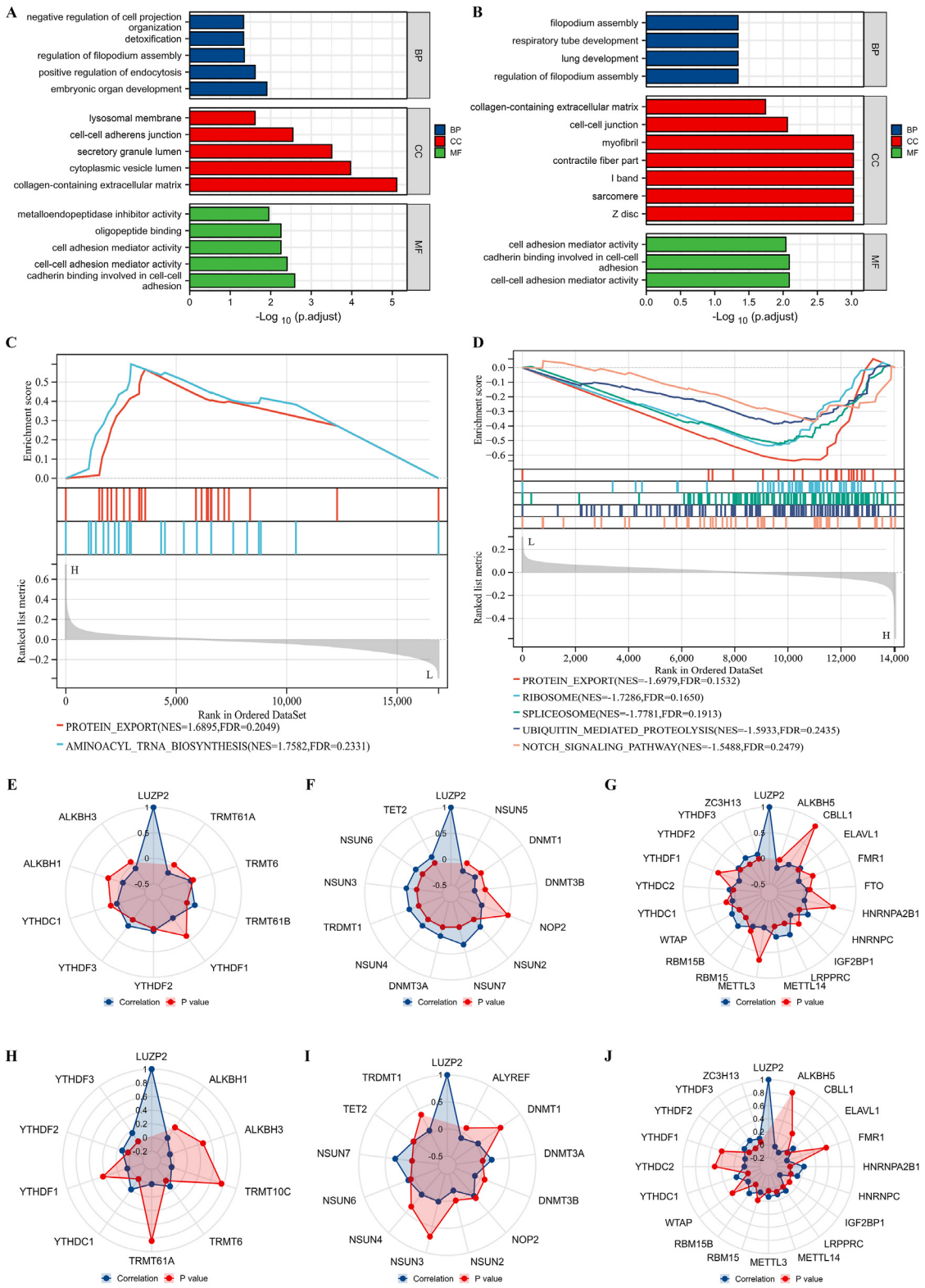

Figure 2. Functional enrichment analysis and RNA modifications (A) the GO analysis results for PCa patients having radical prostatectomy in the TCGA database; (B) the GO analysis results for PCa patients having radical radiotherapy in the GSE116918 [17] (C) the GSEA analysis results for PCa patients having radical prostatectomy in the TCGA database; and (D) the GSEA analysis results for PCa patients having radical radiotherapy in the GSE116918 [17] (E) Radar plots demonstrating the relationship between LUZP2 expression and the m1A marker gene for PCa patients undergoing radical prostatectomy; (F) Radar plots demonstrating the relationship between LUZP2 expression and the m5C marker gene for PCa patients undergoing radical prostatectomy; and (G) Radar plots demonstrating the relationship between LUZP2 expression and the m6A marker gene for PCa patients undergoing radical prostatectomy.; (H) Radar plot demonstrating the correlation of LUZP2 expression with m1A marker genes in PCa patients undergoing radical radiotherapy in the GSE116918 [17]; (I) radar plot demonstrating the correlation of LUZP2 expression with m5C marker genes in PCa patients undergoing radical radiotherapy in the GSE116918 [17]; (J) radar plot demonstrating the correlation of LUZP2 expression with m6A marker genes in PCa patients undergoing radical radiotherapy in the GSE116918 [17]. H = high-expression LUZP2; L = low-expression LUZP2.

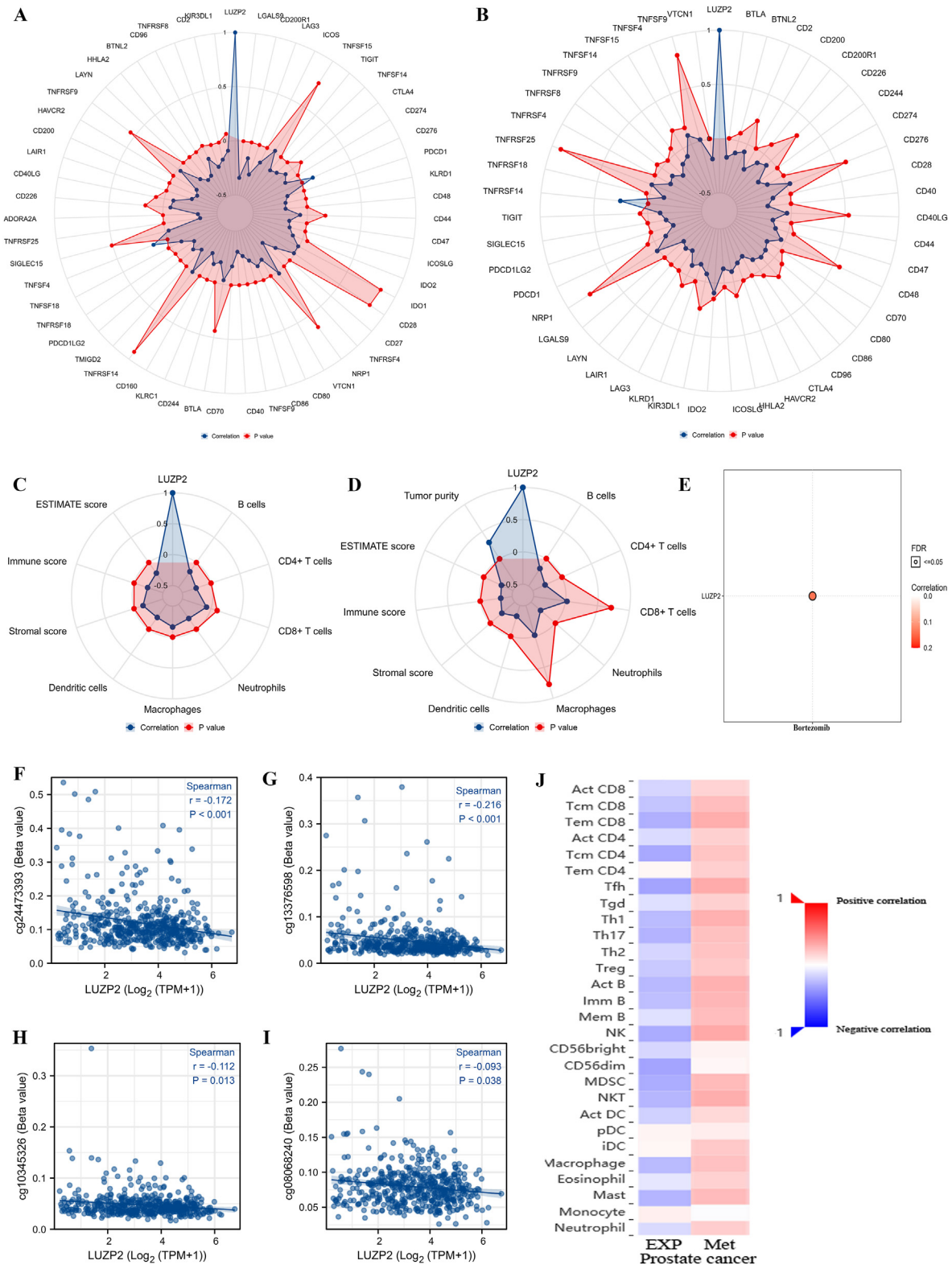

Figure 3. DNA methylation and tumor immune microenvironment (A) radar plot showing the correlation between LUZP2 expression and immune checkpoints for PCa patients undergoing radical prostatectomy in the TCGA database; (B) radar plot showing the correlation between LUZP2 expression and immune checkpoints for PCa patients undergoing radical radiotherapy in the GSE116918 [17] (C) radar plot showing the correlation between LUZP2 expression and immune parameters for PCa patients undergoing radical prostatectomy in the TCGA database; (D) radar plot showing the correlation between LUZP2 expression and immune parameters for PCa patients undergoing radical radiotherapy in the GSE116918 [17] (E) drug sensitivity analysis of LUZP2; (F) the correlation of LUZP2 expression with cg24473393 (G) the correlation of LUZP2 expression with cg213376598; (H) the correlation of LUZP2 expression with cg10345326 (I) the correlation of LUZP2 expression with cg08068240; (J) the correlation of LUZP2 expression and methylation with tumor infiltrating cells. EXP = expression; Met = methylation; PCa = prostate cancer.

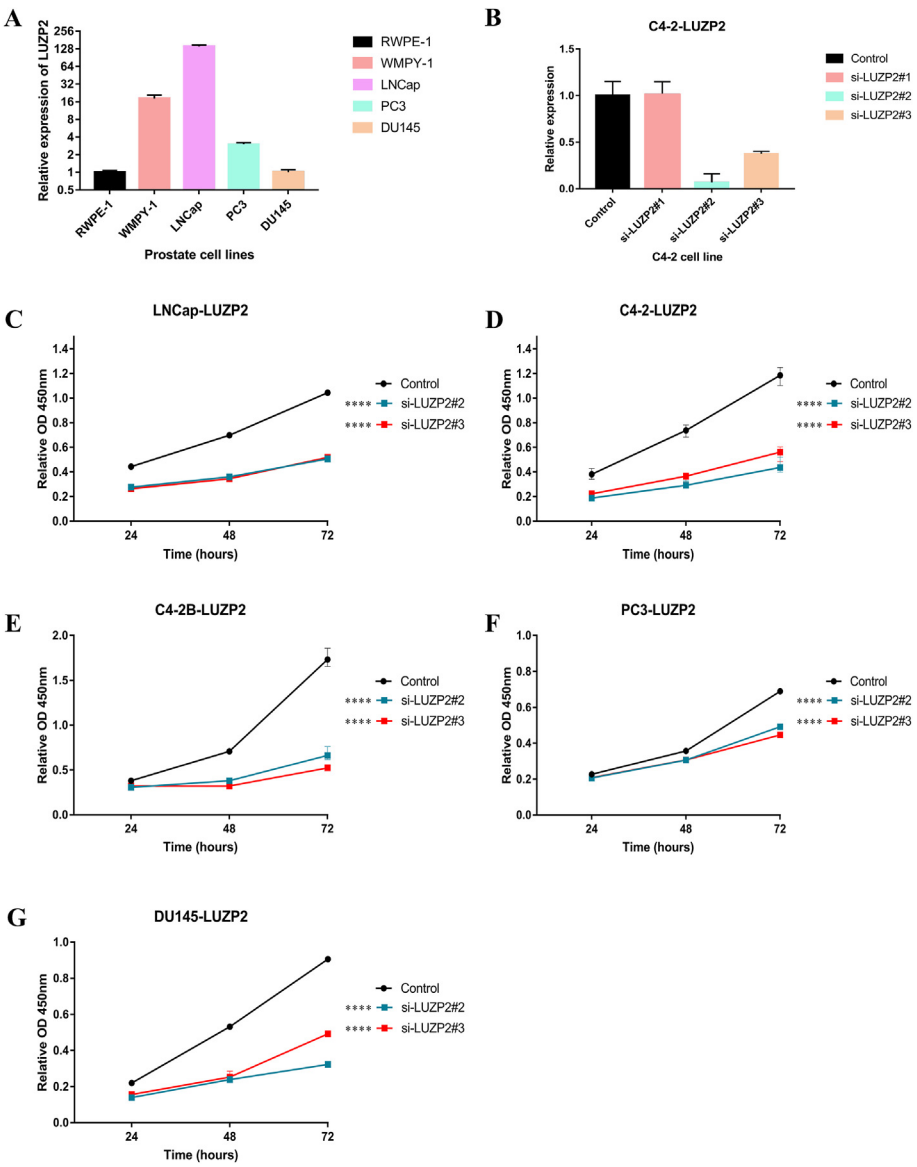

Figure 4. The effect of LUZP2 on biological behaviors of PCa cell lines (A) RT-qPCR results showing the mRNA expression of LUZP2 on tumor and normal prostate cells; (B) RT-qPCR results of LUZP2 siRNAs (C) effect of LUZP2 siRNAs on LNCap using CCK8 assay; (D) effect of LUZP2 siRNAs on C4-2 using CCK8 assay (E) effect of LUZP2 siRNAs on C4–2B using CCK8 assay; (F) effect of LUZP2 siRNAs on PC3 using CCK8 assay; (G) effect of LUZP2 siRNAs on DU145 using CCK8 assay. ****: $p < 0.0001$.

of m6A readers, specifically YTHDF2, can bind to m1A with low affinity, and it has been proposed as a potential m1A reader in cells [81]. In m1A analysis, both RP and RT patients had a positive correlation between LUZP2 and YTHDF3. TRMT6/TRMT61A form a complex that inhibits translation [82]. TRMT61A, on the other hand, was discovered to be negatively correlated with LUZP2 in the RP group, while TRMT6 was discovered to be positively correlated with LUZP2 in the RT group. Furthermore, in the RT group, YTHDF2, which mediates mRNA degradation [83], was positively correlated with LUZP2. Only NSUN2 was associated with mRNA modifications [84], promoting translation [85] among the possible m5C factors we discovered. NSUN2 showed a positive and negative correlation in the RP and RT groups, respectively. We discovered that RNA modification in the RP group was more likely to promote translation, whereas it was more likely to inhibit translation in the RT group. This difference could be due to whether or not the prostate tissue was preserved. Overall, LUZP2 RNA modification inhibits translation and reduces protein production, resulting in less or poor antitumor effects.

We discovered that LUZP2 expression was negatively associated with most immune cells and positively associated with tumor purity, which was consistent with the immune checkpoint analysis. LUZP2 expression was higher in PCa samples than in normal samples, similar to the previous study [16], but overexpression of LUZP2 was significantly associated with better prognosis. As a result, we hypothesized that epigenetic regulation played a role in this phenomenon, which could be supported by the discovery that silencing LUZP2 inhibited the growth of enzalutamide-resistant C4-2 cells [16]. Furthermore, we discovered that DNA methylation could reduce LUZP2 mRNA expression, and the correlations of tumor infiltrating lymphocytes with LUZP2 expression or methylation were inverse, supporting our hypothesis. Overall, we proposed that epigenetic regulation, including RNA modifications and DNA methylation, led to low LUZP2 expression and further promoted TME (immune cells or stroma) and tumor cell senescence, with tumor cell senescence being dominant. Furthermore, we discovered that PCa patients with high-expression LUZP2 who underwent RT had a higher risk of BCR than those who underwent RP. We suspected that radiation-induced senescence played a role in this result [10]. Bortezomib has been shown in previous studies to primarily mediate the ubiquitin-proteasome pathway in the treatment of PCa [86, 87, 88, 89]. We discovered that LUZP2 is also involved in ubiquitin-mediated proteolysis. Furthermore, Zheng et al. [90] discovered that bortezomib inhibited PCa cell proliferation by inducing apoptosis. Bortezomib, which targets LUZP2, could thus be a potential therapeutic.

As the global population ages in the coming decades, PCa in elderly men will pose a significant disease burden. As mutual verification, our study combined two high-throughput sequencing and microarray sequencing platforms, and the identified LUZP2 was more robust. However, the mechanisms underlying immunosenescence and tumor senescence must be investigated further.

5. Conclusions

From the perspective of senescence, we proposed a relatively comprehensive understanding of the roles of LUZP2 on PCa.

Declarations

Author contribution statement

Dechao Feng, Ph. D; Weizhen Zhu, M. D: Conceived and designed the experiments; Performed the experiments; Analyzed and interpreted the data; Contributed reagents, materials, analysis tools or data; Wrote the paper.

Xu Shi, M. D: Conceived and designed the experiments; Analyzed and interpreted the data; Contributed reagents, materials, analysis tools or data; Wrote the paper.

Wuran Wei, Ph. D; Ping Han, Ph. D; Qiang Wei, M. D; Lu Yang, Ph. D: Contributed reagents, materials, analysis tools or data.

Funding statement

This program was supported by the National Natural Science Foundation of China (Grant Nos. 81974099, 82170785, 81974098, 82170784), programs from Science and Technology Department of Sichuan Province (Grant Nos. 2021YFH0172), Young Investigator Award of Sichuan University 2017 (Grant No. 2017SCU04A17), Technology Innovation Research and Development Project of Chengdu Science and Technology Bureau (2019-YF05-00296-SN), Sichuan University–Panzhihua science and technology cooperation special fund (2020 420 CDPZH-4).

Data availability statement

Data included in article/supp. material/referenced in article.

Declaration of interest's statement

The authors declare no conflict of interest.

Additional information

No additional information is available for this paper.

Acknowledgements

The results showed here are in whole or part based upon data generated by the TCGA Research Network: https://www.cancer.gov/tcga.

References

[1] R.L. Siegel, K.D. Miller, H.E. Fuchs, et al., Cancer statistics, 2021, CA A Cancer J. Clin. 71 (1) (2021) 7–33.
[2] E.R. Adelman, H.T. Huang, A. Roisman, et al., Aging human hematopoietic stem cells manifest profound epigenetic reprogramming of enhancers that may predispose to leukemia, Cancer Discov. 9 (8) (2019) 1080–1101.
[3] D. Feng, S. Liu, D. Li, et al., Analysis of conventional versus advanced pelvic floor muscle training in the management of urinary incontinence after radical prostatectomy: a systematic review and meta-analysis of randomized controlled trials, Transl. Androl. Urol. 9 (5) (2020) 2031–2045.
[4] D. Feng, X. Shi, F. Zhang, et al., Energy metabolism-related gene prognostic index predicts biochemical recurrence for patients with prostate cancer undergoing radical prostatectomy, Front. Immunol. 13 (2022), 839362.
[5] D. Feng, X. Shi, Q. Xiong, et al., A ferroptosis-related gene prognostic index associated with biochemical recurrence and radiation resistance for patients with prostate cancer undergoing radical radiotherapy, Front. Cell Dev. Biol. 10 (2022), 803766.
[6] H. Sung, J. Ferlay, R.L. Siegel, et al., Global cancer statistics 2020: GLOBOCAN estimates of incidence and mortality worldwide for 36 cancers in 185 countries, CA A Cancer J. Clin. 71 (3) (2021) 209–249.
[7] D. Feng, X. Shi, Q. Xiong, et al., A gene prognostic index associated with epithelial-mesenchymal transition predicting biochemical recurrence and tumor chemoresistance for prostate cancer, Front. Oncol. 11 (2021), 805571.
[8] A. Calcinotto, J. Kohli, E. Zagato, et al., Cellular senescence: aging, cancer, and injury, Physiol. Rev. 99 (2) (2019) 1047–1078.
[9] J. Freeland, P.D. Crowell, J.M. Giafaglione, et al., Aging of the progenitor cells that initiate prostate cancer, Cancer Lett. 515 (2021 Sep 1) 28–35.
[10] V. Gorgoulis, P.D. Adams, A. Alimonti, et al., Cellular senescence: defining a path forward, Cell 179 (4) (2019) 813–827.
[11] Y. Li, G. Deng, Y. Qi, et al., Downregulation of LUZP2 is correlated with poor prognosis of low-grade glioma, BioMed Res. Int. 2020 (2020), 9716720.
[12] M. Wu, E.J. Michaud, D.K. Johnson, Cloning, functional study and comparative mapping of Luzp2 to mouse chromosome 7 and human chromosome 11p13-11p14, Mamm. Genome 14 (5) (2003) 323–334.
[13] V. Stepanov, K. Vagaitseva, A. Bocharova, et al., Analysis of association of genetic markers in the LUZP2 and FBXO40 genes with the normal variability in cognitive performance in the elderly, Int. J. Alzheimer's Dis. 2018 (2018), 2686045.
[14] A.C. Cummings, L. Jiang, D.R. Velez Edwards, et al., Genome-wide association and linkage study in the Amish detects a novel candidate late-onset Alzheimer disease gene, Ann. Hum. Genet. 76 (5) (2012) 342–351.
[15] Schizophrenia Working Group of the Psychiatric Genomics Consortium, Biological insights from 108 schizophrenia-associated genetic loci, Nature 511 (7510) (2014) 421–427.
[16] J. Zhao, Y. Zhao, L. Wang, et al., Alterations of androgen receptor-regulated enhancer RNAs (eRNAs) contribute to enzalutamide resistance in castration-resistant prostate cancer, Oncotarget 7 (25) (2016) 38551–38565.
[17] D. Feng, X. Shi, F. Zhang, et al., Mitochondria dysfunction-mediated molecular subtypes and gene prognostic index for prostate cancer patients undergoing radical prostatectomy or radiotherapy, Front. Oncol. 12 (2022), 858479.
[18] J. Taminau, S. Meganck, C. Lazar, et al., Unlocking the potential of publicly available microarray data using inSilicoDb and inSilicoMerging R/Bioconductor packages, BMC Bioinf. 13 (2012) 335.
[19] M.M. Mortensen, S. Høyer, A.S. Lynnerup, et al., Expression profiling of prostate cancer tissue delineates genes associated with recurrence after prostatectomy, Sci. Rep. 5 (2015), 16018.
[20] R. Kuner, M. Fälth, N.C. Pressinotti, et al., The maternal embryonic leucine zipper kinase (MELK) is upregulated in high-grade prostate cancer, J. Mol. Med. (Berl.) 91 (2) (2013) 237–248.
[21] K.L. Penney, J.A. Sinnott, S. Tyekucheva, et al., Association of prostate cancer risk variants with gene expression in normal and tumor tissue, Cancer Epidemiol. Biomarkers Prev. 24 (1) (2015) 255–260.
[22] S. Jain, C.A. Lyons, S.M. Walker, et al., Validation of a Metastatic Assay using biopsies to improve risk stratification in patients with prostate cancer treated with radical radiation therapy, Ann. Oncol. 29 (1) (2018) 215–222.
[23] M.J. Goldman, B. Craft, M. Hastie, et al., Visualizing and interpreting cancer genomics data via the Xena platform, Nat. Biotechnol. 38 (6) (2020) 675–678.
[24] T. Li, J. Fu, Z. Zeng, et al., TIMER2.0 for analysis of tumor-infiltrating immune cells, Nucleic Acids Res. 48 (W1) (2020) W509–W514.
[25] G. Yu, L.G. Wang, Y. Han, et al., clusterProfiler: an R package for comparing biological themes among gene clusters, OMICS A J. Integr. Biol. 16 (5) (2012) 284–287.
[26] A. Liberzon, A. Subramanian, R. Pinchback, et al., Molecular signatures database (MSigDB) 3.0, Bioinformatics 27 (12) (2011) 1739–1740.
[27] B. Li, E. Severson, J.C. Pignon, et al., Comprehensive analyses of tumor immunity: implications for cancer immunotherapy, Genome Biol. 17 (1) (2016) 174.
[28] K. Yoshihara, M. Shahmoradgoli, E. Martínez, et al., Inferring tumour purity and stromal and immune cell admixture from expression data, Nat. Commun. 4 (2013) 2612.
[29] C.J. Liu, F.F. Hu, M.X. Xia, et al., GSCALite: a web server for gene set cancer analysis, Bioinformatics 34 (21) (2018) 3771–3772.
[30] B. Ru, C.N. Wong, Y. Tong, et al., TISIDB: an integrated repository portal for tumor-immune system interactions, Bioinformatics 35 (20) (2019) 4200–4202.
[31] J. Campisi, Aging, cellular senescence, and cancer, Annu. Rev. Physiol. 75 (2013) 685–705.
[32] T. Alber, Structure of the leucine zipper, Curr. Opin. Genet. Dev. 2 (2) (1992) 205–210.
[33] G. Stelzer, N. Rosen, I. Plaschkes, et al., The GeneCards suite: from gene data mining to disease genome sequence analyses, Curr Protoc Bioinformatics 54 (2016) 1–1.30.33.
[34] H. Li, Y. Zhang, D. Li, et al., Androgen receptor splice variant 7 predicts shorter response in patients with metastatic hormone-sensitive prostate cancer receiving androgen deprivation therapy, Eur. Urol. 79 (6) (2021 Jun) 879–886.
[35] L. Fagerberg, B.M. Hallström, P. Oksvold, et al., Analysis of the human tissue-specific expression by genome-wide integration of transcriptomics and antibody-based proteomics, Mol. Cell. Proteomics 13 (2) (2014 Feb) 397–406.

[36] R. Makboul, I.F. Abdelkawi, D.M. Badary, et al., Transmembrane and tetratricopeptide repeat containing 4 is a novel diagnostic marker for prostate cancer with high specificity and sensitivity, Cells 10 (5) (2021).
[37] C.D.C. Kamilaris, F. Hannah-Shmouni, C.A. Stratakis, Adrenocortical tumorigenesis: lessons from genetics, Best Pract. Res. Clin. Endocrinol. Metabol. 34 (3) (2020), 101428.
[38] C.Y. Wang, M.D. Lai, N.N. Phan, et al., Meta-analysis of public microarray datasets reveals voltage-gated calcium gene signatures in clinical cancer patients, PLoS One 10 (7) (2015), e0125766.
[39] Q. Luo, Y. Liu, Z. Yuan, et al., Expression of Rab3b in human glioma: influence on cell proliferation and apoptosis, Curr. Pharmaceut. Des. 27 (7) (2021) 989–995.
[40] O. Mijanovic, A. Brankovic, A.N. Panin, et al., Cathepsin B: a sellsword of cancer progression, Cancer Lett. 449 (2019) 207–214.
[41] D. Wang, L. Zhu, M. Liao, et al., MYO6 knockdown inhibits the growth and induces the apoptosis of prostate cancer cells by decreasing the phosphorylation of ERK1/2 and PRAS40, Oncol. Rep. 36 (3) (2016) 1285–1292.
[42] S. Al Bashir, M. Alshalalfa, S.A. Hegazy, et al., Cysteine- rich secretory protein 3 (CRISP3), ERG and PTEN define a molecular subtype of prostate cancer with implication to patients' prognosis, J. Hematol. Oncol. 7 (2014) 21.
[43] N.B. Griner, D. Young, P. Chaudhary, et al., ERG oncoprotein inhibits ANXA2 expression and function in prostate cancer, Mol. Cancer Res. 13 (2) (2015) 368–379.
[44] J. Munkley, Glycosylation is a global target for androgen control in prostate cancer cells, Endocr. Relat. Cancer 24 (3) (2017) R49–R64.
[45] X.M. Piao, B. Hwang, P. Jeong, et al., Collagen type VI-α1 and 2 repress the proliferation, migration and invasion of bladder cancer cells, Int. J. Oncol. 59 (1) (2021) 37.
[46] T. Acun, K.M. Senses, Downregulation of DNAJC10 (ERDJ5) is associated with poor survival in breast cancer, Breast Cancer 27 (3) (2020) 483–489.
[47] Q. Chen, Y.T. Yao, H. Xu, et al., SPOCK1 promotes tumor growth and metastasis in human prostate cancer, Drug Des. Dev. Ther. 10 (2016) 2311–2321.
[48] W. Yan, M. Jamal, S.H. Tan, et al., Molecular profiling of radical prostatectomy tissue from patients with no sign of progression identifies ERG as the strongest independent predictor of recurrence, Oncotarget 10 (60) (2019) 6466–6483.
[49] M. Uegaki, Y. Kita, R. Shirakawa, et al., Downregulation of RalGTPase-activating protein promotes invasion of prostatic epithelial cells and progression from intraepithelial neoplasia to cancer during prostate carcinogenesis, Carcinogenesis 40 (12) (2019) 1535–1544.
[50] H. Yamaguchi, J. Wyckoff, J. Condeelis, Cell migration in tumors, Curr. Opin. Cell Biol. 17 (5) (2005) 559–564.
[51] Y. Lai, F. Tang, Y. Huang, et al., The tumour microenvironment and metabolism in renal cell carcinoma targeted or immune therapy, J. Cell. Physiol. 236 (3) (2021) 1616–1627.
[52] A.J. Ridley, M.A. Schwartz, K. Burridge, et al., Cell migration: integrating signals from front to back, Science 302 (5651) (2003) 1704–1709.
[53] R. Buccione, J.D. Orth, M.A. McNiven, Foot and mouth: podosomes, invadopodia and circular dorsal ruffles, Nat. Rev. Mol. Cell Biol. 5 (8) (2004) 647–657.
[54] H. Yamaguchi, M. Lorenz, S. Kempiak, et al., Molecular mechanisms of invadopodium formation: the role of the N-WASP-Arp2/3 complex pathway and cofilin, J. Cell Biol. 168 (3) (2005) 441–452.
[55] K. Augoff, A. Hryniewicz-Jankowska, R. Tabola, Invadopodia: clearing the way for cancer cell invasion, Ann. Transl. Med. 8 (14) (2020) 902.
[56] M.F. Olson, E. Sahai, The actin cytoskeleton in cancer cell motility, Clin. Exp. Metastasis 26 (4) (2009) 273–287.
[57] D. Liu, X.Y. Qiu, X. Wu, et al., Piperlongumine suppresses bladder cancer invasion via inhibiting epithelial mesenchymal transition and F-actin reorganization, Biochem. Biophys. Res. Commun. 494 (1-2) (2017) 165–172.
[58] D.R. Millard Jr., S. Berkowitz, R.A. Latham, et al., A discussion of presurgical orthodontics in patients with clefts, Cleft Palate J. 25 (4) (1988) 403–412.
[59] D. Xiong, Y.L. Ye, M.K. Chen, et al., Non-muscle myosin II is an independent predictor of overall survival for cystectomy candidates with early-stage bladder cancer, Oncol. Rep. 28 (5) (2012) 1625–1632.
[60] H. Yu, Z. Zhu, J. Chang, et al., Lentivirus-mediated silencing of myosin VI inhibits proliferation and cell cycle progression in human lung cancer cells, Chem. Biol. Drug Des. 86 (4) (2015) 606–613.
[61] R. Kong, F. Yi, P. Wen, et al., Myo9b is a key player in SLIT/ROBO-mediated lung tumor suppression, J. Clin. Invest. 125 (12) (2015) 4407–4420.
[62] X. Yang, H. Ren, X. Guo, et al., The expressions and mechanisms of sarcomeric proteins in cancers, Dis. Markers 2020 (2020), 8885286.
[63] S. Hirohashi, Y. Kanai, Cell adhesion system and human cancer morphogenesis, Cancer Sci. 94 (7) (2003) 575–581.
[64] J. Wang, X.L. Yang, Novel functions of cytoplasmic aminoacyl-tRNA synthetases shaping the hallmarks of cancer, Enzymes 48 (2020) 397–423.
[65] M. Guo, P. Schimmel, Essential nontranslational functions of tRNA synthetases, Nat. Chem. Biol. 9 (3) (2013) 145–153.
[66] X. Deschênes-Simard, F. Lessard, M.F. Gaumont-Leclerc, et al., Cellular senescence and protein degradation: breaking down cancer, Cell Cycle 13 (12) (2014) 1840–1858.
[67] M. Hoare, M. Narita, NOTCH and the 2 SASPs of senescence, Cell Cycle 16 (3) (2017) 239–240.
[68] Y.V. Teo, N. Rattanavirotkul, N. Olova, et al., Notch signaling mediates secondary senescence, Cell Rep. 27 (4) (2019) 997–1007, e5.
[69] M. Hoare, M. Narita, Notch and senescence, Adv. Exp. Med. Biol. 1066 (2018) 299–318.
[70] B.S. Zhao, I.A. Roundtree, C. He, Post-transcriptional gene regulation by mRNA modifications, Nat. Rev. Mol. Cell Biol. 18 (1) (2017) 31–42.
[71] Y. Yang, P.J. Hsu, Y.S. Chen, et al., Dynamic transcriptomic m(6)A decoration: writers, erasers, readers and functions in RNA metabolism, Cell Res. 28 (6) (2018) 616–624.
[72] S.K. Kota, Z.W. Lim, S.B. Kota, Elavl1 impacts osteogenic differentiation and mRNA levels of genes involved in ECM organization, Front. Cell Dev. Biol. 9 (2021), 606971.
[73] P. Loyer, A. Busson, J.H. Trembley, et al., The RNA binding motif protein 15B (RBM15B/OTT3) is a functional competitor of serine-arginine (SR) proteins and antagonizes the positive effect of the CDK11p110-cyclin L2α complex on splicing, J. Biol. Chem. 286 (1) (2011) 147–159.
[74] N. Liu, Q. Dai, G. Zheng, et al., N(6)-methyladenosine-dependent RNA structural switches regulate RNA-protein interactions, Nature 518 (7540) (2015) 560–564.
[75] X.L. Ping, B.F. Sun, L. Wang, et al., Mammalian WTAP is a regulatory subunit of the RNA N6-methyladenosine methyltransferase, Cell Res. 24 (2) (2014) 177–189.
[76] P.J. Hsu, Y. Zhu, H. Ma, et al., Ythdc2 is an N(6)-methyladenosine binding protein that regulates mammalian spermatogenesis, Cell Res. 27 (9) (2017) 1115–1127.
[77] C. Gu, Z. Wang, N. Zhou, et al., Mettl14 inhibits bladder TIC self-renewal and bladder tumorigenesis through N(6)-methyladenosine of Notch1, Mol. Cancer 18 (1) (2019) 168.
[78] J. Zhou, J. Wan, X. Gao, et al., Dynamic m(6)A mRNA methylation directs translational control of heat shock response, Nature 526 (7574) (2015) 591–594.
[79] I. Barbieri, T. Kouzarides, Role of RNA modifications in cancer, Nat. Rev. Cancer 20 (6) (2020) 303–322.
[80] C.R. Alarcón, H. Goodarzi, H. Lee, et al., HNRNPA2B1 is a mediator of m(6)a-dependent nuclear RNA processing events, Cell 162 (6) (2015) 1299–1308.
[81] X. Dai, T. Wang, G. Gonzalez, et al., Identification of YTH domain-containing proteins as the readers for N1-methyladenosine in RNA, Anal. Chem. 90 (11) (2018) 6380–6384.
[82] M. Safra, A. Sas-Chen, R. Nir, et al., The m1A landscape on cytosolic and mitochondrial mRNA at single-base resolution, Nature 551 (7679) (2017) 251–255.
[83] H. Du, Y. Zhao, J. He, et al., YTHDF2 destabilizes m(6)A-containing RNA through direct recruitment of the CCR4-NOT deadenylase complex, Nat. Commun. 7 (2016), 12626.
[84] K.E. Bohnsack, C. Höbartner, M.T. Bohnsack, Eukaryotic 5-methylcytosine (m^5C) RNA methyltransferases: mechanisms, cellular functions, and links to disease, Genes 10 (2) (2019).
[85] J. Xing, J. Yi, X. Cai, et al., NSun2 promotes cell growth via elevating cyclin-dependent kinase 1 translation, Mol. Cell Biol. 35 (23) (2015) 4043–4052.
[86] E. Kanbur, Baykal AT, and Yerlikaya A Molecular analysis of cell survival and death pathways in the proteasome inhibitor bortezomib-resistant PC3 prostate cancer cell line, Med. Oncol. 38 (9) (2021) 112.
[87] A. Sato, T. Asano, K. Ito, et al., Vorinostat and bortezomib synergistically cause ubiquitinated protein accumulation in prostate cancer cells, J. Urol. 188 (6) (2012) 2410–2418.
[88] K. Tsapakidis, P.J. Vlachostergios, I.A. Voutsadakis, et al., Bortezomib reverses the proliferative and antiapoptotic effect of neuropeptides on prostate cancer cells, Int. J. Urol. 19 (6) (2012) 565–574.
[89] Z. Wang, J. Wang, X. Li, et al., Bortezomib prevents oncogenesis and bone metastasis of prostate cancer by inhibiting WWP1, Smurf1 and Smurf2, Int. J. Oncol. 45 (4) (2014) 1469–1478.
[90] R.P. Zheng, W. Wang, C.D. Wei, Bortezomib inhibits cell proliferation in prostate cancer, Exp. Ther. Med. 10 (3) (2015) 1219–1223.